STS properties of defective metallic carbon nanotubes

2000 J. Phys.: Condens. Matter 12 8617

(http://iopscience.iop.org/0953-8984/12/40/306)

J. Phys.: Condens. Matter **12** (2000) 8617–8622. Printed in the UK PII: S0953-8984(00)15569-9

STS properties of defective metallic carbon nanotubes

Feng Wei†, Jia-Lin Zhu†‡ and Hao-Ming Chen†

† Department of Physics, Tsinghua University, Beijing 100084, People's Republic of China
‡ Center for Advanced Study, Tsinghua University, Beijing 100084, People's Republic of China

Received 11 July 2000, in final form 29 August 2000

Abstract. The influence of point defects on the scanning tunnelling spectroscopic property of metallic carbon nanotubes is studied theoretically. The tight-binding model and Green's function method are applied to simulate the local density of states. A resonant state is induced by a strong defect which depends on the nanotube diameter rather than chirality. The corresponding spectroscopic image shows a highly localized state around the defect and gives some unique characteristics of point defects. The local density of states image is found to relate to the nanotube chirality.

1. Introduction

Since Iijima's observation in 1991 [1], carbon nanotubes have been the subject of an increasing number of experimental and theoretical studies due to their quasi-one-dimensional structure and unique electronic property [2]. Among the detecting techniques, scanning tunnelling microscopy (STM), and in particular, scanning tunnelling spectroscopy (STS) may be very powerful tools with which to investigate not only the morphology of individual carbon nanotubes, but also the electronic properties. Previous STM and STS studies [3, 4] have confirmed the prediction [5] that carbon nanotubes can be metallic or semiconducting depending on the tube diameter and chiral angle between the tube axis and hexagon rows in the atomic lattice. The electron standing waves in finite-size metallic carbon nanotubes [6] and the electronic properties of capped, doped, and connected tubes [7, 8] have recently been studied by STM and STS.

The theoretical works on STM and STS properties mainly concerned defects on nanotubes both in the absence and presence of additional carbon atoms [9, 10]. Orlikowski *et al* [10], for instance, have calculated that there would be a set of bright rings in the STM images, whose positions correlate with the location of the pentagons within the defect. Other kinds of topological defects, such as point defects, which represent incomplete bonding [11] also have a significant effect on the electric properties of carbon nanotubes. Current calculations of transport properties have suggested that the point defects are of great importance in the one-dimensional systems which can induce a considerable amount of scattering [12, 13]. Therefore, it is interesting to show how the defects influence the electronic structure which relate to transport properties. We believe that the STM and STS will remain the primary means of actually identifying and visualizing the defects.

In this paper, we investigate the influence of point defects on the electrical local density of states (LDOS) that is proportional to the differential conductance $\mathrm{d}I/\mathrm{d}V$ detected in STS [14]. The tight-binding (TB) model and the Green's function method have been used to accomplish

0953-8984/00/408617+06$30.00

the calculation, since it is proved to be valid for states a few tenths of an eV above or below the Fermi level by previous *ab initio* calculations [15]. We find that a resonant state is induced at the defective point. The position and width of the resonant state are expressed in terms of two universal relationships depending only on the nanotube diameter which is verified by numerical calculations. The analytical results provide a reference by which to discuss more complex and realistic defects in carbon nanotubes. The LDOS around the defect are also mapped which show a highly localized state and the chirality is embodied in these images. Though many of the defects are quite complex, and the interactions stemming from tube packing or the tube/substrate/tip [16, 17] make the explanation more involuted, the LDOS properties of point defects will hopefully provide an important guide for experimental investigation.

2. Formulation

The metallic carbon nanotubes with one point defect at the A or B sublattice site are studied. The total Hamiltonian is as follows

$$H = H_0 + H_{def} \tag{1}$$

where H_0 are the electronic states of defect-free carbon nanotubes based on the π-electron TB model [18], and H_{def} is the point defect.

The two Bloch functions, constructed from atomic orbitals for the two inequivalent carbon atoms at sites A and B, provide the basis functions for single-walled carbon nanotubes (SWCNT) as well as for two-dimensional graphite. The Hamiltonian in the secondly quantized representation has the following form

$$H_0 = \sum_{\boldsymbol{k}} \Psi_{\boldsymbol{k}}^{+} E_{\boldsymbol{k}} \Psi_{\boldsymbol{k}} \tag{2}$$

where $\Psi_{\boldsymbol{k}}$ is an annihilation operator with two components:

$$\Psi_{\boldsymbol{k}} = \begin{pmatrix} C_{\boldsymbol{k}A} \\ C_{\boldsymbol{k}B} \end{pmatrix}.$$

$C_{\boldsymbol{k}A}$ and $C_{\boldsymbol{k}B}$ are for the A and B Bloch functions, separately. $\boldsymbol{k}$ covers the Brillouin zone (BZ) of the carbon nanotube. $E_{\boldsymbol{k}}$ is an energy matrix:

$$E_{\boldsymbol{k}} = \begin{pmatrix} 0 & \gamma_0 f(\boldsymbol{k}) \\ \gamma_0 f^*(\boldsymbol{k}) & 0 \end{pmatrix} \tag{3}$$

where $\gamma_0 (\sim -2.5\,\text{eV})$ is the nearest-neighbour interaction. $f(\boldsymbol{k})$ is the sum of the phase factor of $e^{i\boldsymbol{k}\cdot\boldsymbol{R}_j}$ ($j = 1, 2, 3$) with R_j the three nearest-neighbour B atoms relative to an A atom, and $*$ denotes the complex conjugate.

The second term in equation (1) is the point defect

$$H_{def} = \left(\frac{2}{N_s}\right) \sum_{\boldsymbol{k},\boldsymbol{k}'} \Psi_{\boldsymbol{k}}^{+} U \Psi_{\boldsymbol{k}'} \tag{4}$$

where N_s is the total lattice number. U is the defect matrix:

$$U = \begin{pmatrix} V_{def} & 0 \\ 0 & 0 \end{pmatrix} \tag{5}$$

with V_{def} the defect strength. Here we assume that the defect is at an A site.

The propagator of the electrons on the nanotube is defined in the matrix form

$$G_{\boldsymbol{k},\boldsymbol{k}'}(\tau, \tau') = -\langle T_\tau \Psi_{\boldsymbol{k}}(\tau) \Psi_{\boldsymbol{k}}^{+}(\tau') \rangle \tag{6}$$

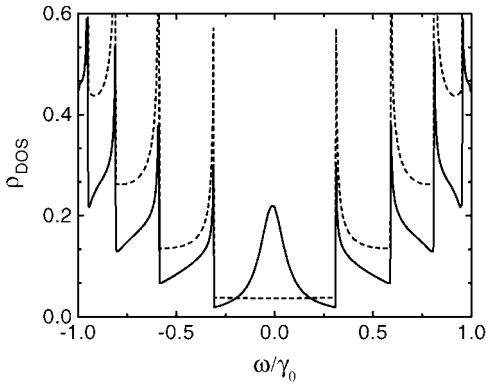

Figure 1. The DOS at the defect point in an armchair (10, 10) nanotube with defect strength $100\gamma_0$. The full curve shows the DOS of the defective nanotube, while the broken curve is the DOS of a perfect one. A resonant state appears at $\omega = -0.012\gamma_0$ in contrast to the metallic plateau for a perfect nanotube.

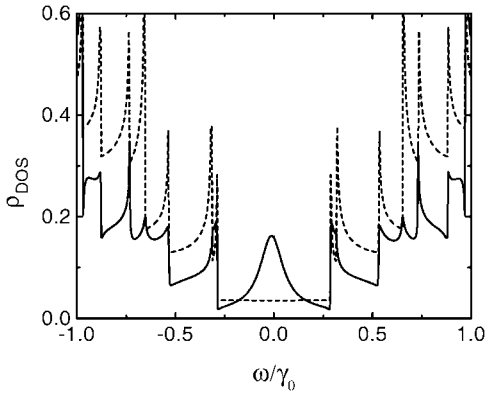

Figure 2. The same as in figure 1 for a zigzag (18, 0) nanotube.

where T_τ is the time ordering operator with respect to the imaginary time τ and $\Psi_{\boldsymbol{k}}(\tau) = \exp(H\tau)\Psi_{\boldsymbol{k}}\exp(-H\tau)$. The Fourier transformation of G is calculated as

$$\mathrm{i}\omega_n G_{\boldsymbol{k},\boldsymbol{k}'}(\mathrm{i}\omega_n) = \delta_{\boldsymbol{k},\boldsymbol{k}'} + G_{\boldsymbol{k},\boldsymbol{k}'}(\mathrm{i}\omega_n)E_{\boldsymbol{k}'} + \left(\frac{2}{N_s}\right)\sum_{\boldsymbol{k}''} G_{\boldsymbol{k},\boldsymbol{k}''}(\mathrm{i}\omega_n)U \tag{7}$$

where ω_n is the odd Matsubara frequency for fermions. The retarded Green's function can be obtained from equation (7) by changing $\mathrm{i}\omega_n$ to $\omega + \mathrm{i}0^+$ which is called an analytic continuation [19]. To discuss the LDOS property, we transform the Green's function from $\boldsymbol{k}$ space to real space

$$G_{ret}(\boldsymbol{r}, \boldsymbol{r}', \omega) = G^{(0)}_{ret}(\boldsymbol{r}, \omega) + G^{(0)}_{ret}(\boldsymbol{r}, \omega)\left(\frac{1}{1 - UG^{(0)}_{ret}(0, \omega)}U\right)G^{(0)}_{ret}(-\boldsymbol{r}', \omega^+). \tag{8}$$

Define

$$T(\omega) = \frac{1}{1 - UG^{(0)}_{ret}(0, \omega)}U. \tag{9}$$

The LDOS can be expressed as:

$$\rho_{LDOS}(\boldsymbol{r}, \omega) = -\frac{1}{\pi}\mathrm{Im}\,[Tr(G_{ret}(\boldsymbol{r}, \boldsymbol{r}, \omega)]. \tag{10}$$

Note all the above ω represent $\omega + \mathrm{i}0^+$. Here the detailed structure of the atomic wavefunction is not considered as the previous experiment [6] suggests that the lattice periodicity is largely compensated when the STM tip follows the atomic corrugation by scanning in constant-current mode in order to map the local density of states.

3. Results and discussion

Two metallic carbon nanotubes, the armchair (10, 10) and the zigzag (18, 0), with diameter 1.3–1.4 nm, have been investigated. We study a single vacancy which can be simulated as an extremely strong defect, about $10^8 \times \gamma_0$, according to [13]. However, to explain the results

credibly, we have the defect strength $100\gamma_0$ and as we will see below, the STS properties of defect strengths $100\gamma_0$ and $10^8 \times \gamma_0$ are of little difference. The full curve in figure 1 shows the density of states (DOS) at the defect-present point of the defective (10, 10) nanotube in contrast with the dashed curve which is the DOS of the perfect one. Figure 2 is for the (18, 0) nanotube. In both graphs, a resonant state appears near the Fermi energy $\varepsilon = 0$ where it is originally a metallic plateau for a perfect nanotube. According to equation (8), the extremum of $T(\omega)$ determines where the resonant state is. We write its component explicitly as

$$T(\omega) = \frac{1}{1/V_{def} - (2/N_s)\sum_{\boldsymbol{k}}(\omega/(\omega^2 - \gamma_0^2|f(\boldsymbol{k})|^2))} \begin{pmatrix} 1 & 0 \\ 0 & 0 \end{pmatrix} \tag{11}$$

noting that ω represents $\omega + \mathrm{i}0^+$.

Accordingly the zero of

$$\frac{1}{V_{def}} - \mathrm{Re}\left(\frac{2}{N_s}\sum_{\boldsymbol{k}}\frac{\omega}{\omega^2 - \gamma_0^2|f(\boldsymbol{k})|^2}\right)$$

determines the energy of the resonance solution. The real part of

$$\frac{2}{N_s}\sum_{\boldsymbol{k}}\frac{\omega}{\omega^2 - \gamma_0^2|f(\boldsymbol{k})|^2}$$

can be related to its imaginary part through the Kramers–Kronig relations

$$\mathrm{Re}\left(\frac{2}{N_s}\sum_{\boldsymbol{k}}\frac{\omega}{\omega^2 - \gamma_0^2|f(\boldsymbol{k})|^2}\right) = \frac{1}{\pi}\int_{-\infty}^{\infty}\mathrm{d}\omega'\,\mathrm{Im}\left(\frac{2}{N_s}\sum_{\boldsymbol{k}}\frac{\omega}{\omega^2 - \gamma_0^2|f(\boldsymbol{k})|^2}\right)P\frac{1}{\omega' - \omega}. \tag{12}$$

According to equations (8) and (10), the imaginary part is proportional to the DOS of the perfect nanotube:

$$\mathrm{Im}\left(\frac{2}{N_s}\sum_{\boldsymbol{k}}\frac{\omega}{\omega^2 - \gamma_0^2|f(\boldsymbol{k})|^2}\right) = -\frac{\pi}{2}\rho_0(\omega). \tag{13}$$

$\rho_0(\omega)$ is estimated from [20] which gives a universal relationship

$$\rho_0(\omega) = \frac{2}{\pi}\frac{1}{|\gamma_0|}\frac{a}{L}\sum_{l=-\infty}^{\infty} g(\omega, \varepsilon_l) \tag{14}$$

where a is the lattice constant of two-dimensional graphite, L is the length of circumference, and

$$\varepsilon_l = \frac{\pi}{\sqrt{3}}|\gamma_0|\frac{a}{L}|3l| \tag{15}$$

$$g(\omega, \varepsilon_l) = \begin{cases} |\omega|/\sqrt{\omega^2 - \varepsilon_l^2} & |\omega| > \varepsilon_l \\ 0 & |\omega| < \varepsilon_l. \end{cases} \tag{16}$$

For energies $\omega \ll \sqrt{3}\pi|\gamma_0|a/L$, considering first-order approximation, the real part can be written as

$$\mathrm{Re}\left(\frac{2}{N_s}\sum_{\boldsymbol{k}}\frac{\omega}{\omega^2 - \gamma_0^2|f(\boldsymbol{k})|^2}\right) = -\frac{\omega}{|\gamma_0|^2}\left\{\frac{4\sqrt{3}}{\pi^2}\sum_{n=1}^{N}\left[\frac{\pi}{6n} - \frac{1}{3n}\arcsin\left(\frac{n}{N}\right)\right] + \frac{2}{3}\frac{a}{\pi L}\right\} \tag{17}$$

with N the nearest integer to $(\sqrt{3}/\pi)(L/a)$. Equation (17) can be simplified as

$$\mathrm{Re}\left(\frac{2}{N_s}\sum_{\boldsymbol{k}}\frac{\omega}{\omega^2 - \gamma_0^2|f(\boldsymbol{k})|^2}\right) = c\omega/|\gamma_0|^2.$$

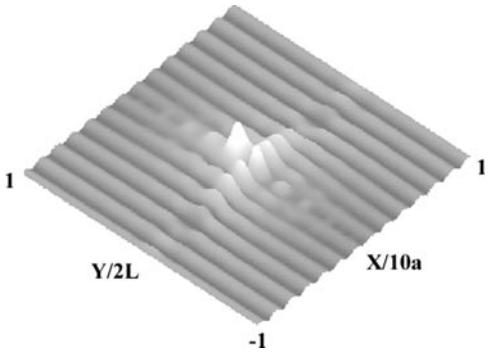

Figure 3. Local density of states (in grey scale) against the position along the circumferential direction (y-axis) and translational direction (x-axis) at the resonant state energy for a (10, 10) nanotube.

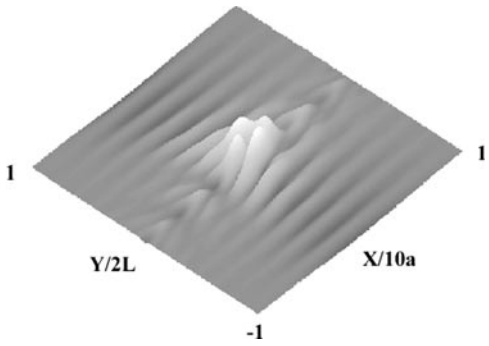

Figure 4. The same as in figure 3 for a (18, 0) nanotube.

For the two nanotubes of diameter 1.3–1.4 nm, the proportional coefficient c is about -0.8–-0.9 which is in good agreement with the numerical integral in the range $[-0.3\gamma_0, 0.3\gamma_0]$. When V_{def} is of the value $100\gamma_0$, the resonant state energy is $-0.012\gamma_0$ which can be testified in the two graphs. For larger V_{def}, the resonant state energy is closer to zero, and the essential STS properties are the same. The position of the resonance state can be obtained in experiments by adjusting the bias voltage between the STM tip and samples. Next, equation (11) is examined again to find the state width. From equations (13) and (14), the imaginary part is a constant of the value $-a/L|\gamma_0|$in the region $|\omega| < \sqrt{3}\pi|\gamma_0|a/L$, therefore, the width of the resonant state is

$$\Gamma = \frac{2a}{cL}|\gamma_0| \tag{18}$$

with the value about $0.13|\gamma_0|$–$0.14|\gamma_0|$ which is consistent with that in figures 1 and 2. In metallic tubes, the defect-induced resonant state energy and the state width completely depend on tube diameter while tube chirality is trivial. What is more, the state width is a constant for large defect strength. The peak of the differential conductance was also observed in other works, such as [10] and [21].

Figures 3 and 4 depict the LDOS around the defect point at the resonant state energy for an armchair (10, 10) and zigzag (18, 0), respectively. As already mentioned, under the constant-current scanning mode, the localized state can be resolved in the spectroscopy measurements because the lattice periodicity is largely compensated when the STM tip follows the atomic corrugation [6]. In the two graphs the length of $20a$ along the translational direction and the whole circumference around the defect are mapped. The LDOS decays rapidly along both directions which confirms that a localized state appears at the resonant energy. Additionally, there is a fluctuation of the periodicity of about $1.5a$ along the translational direction for the armchair nanotube while along the circumferential direction for the zigzag nanotube. The quantity LDOS is a measure of the squared amplitude of the localized electron wavefunction $|\Psi(\boldsymbol{r})|^2$ expressed as:

$$\rho_{LDOS}(\boldsymbol{r}, \omega) = \sum_i |\Psi_i(\boldsymbol{r})|^2 \delta(E_i - E) \tag{19}$$

where Ψ_i and E_i are the electron wavefunction and the eigenvalue of state i, respectively. Since the resonant energy is close to the Fermi energy, the wavevector is nearly the Fermi wavevector $|\boldsymbol{k}_F| = 2\pi/3a$. What is more, $\boldsymbol{k}_F$ is in the translational direction for armchair

nanotubes, in the circumferential direction for the zigzag and has magnitude in both directions for other types of metallic nanotubes [22]. Equation (19) indicates that the LDOS periodicity is half of the Fermi wavelength.

In summary, a study of the STS of metallic carbon nanotubes with large strength point defect have been presented. Within a simple TB model the Green's function of an armchair and zigzag nanotube was calculated. Through an analytic treatment, the defect-induced resonant state was found to be determined by the nanotube diameter rather than chirality. The numerically simulant STS verified the localized state in real space. This suggests that the STM and STS can provide more details with which to identify the type and position of defects in contrast to other measurements such as the conductance signature. It is believed that the experiments necessary to obtain detailed information about the defects of carbon nanotubes should become achievable before long, with the aid of nanomanipulators and other such devices [23, 24]. Theoretical investigations are indispensable in explaining the results. In order to reach a full understanding of the effects of defects, it is necessary to carry on more precise calculations and consider a variety of defects.

Acknowledgment

The financial support from NSF-China (Grant no 19974019) and China's '973' program is gratefully acknowledged.

References

[1] Iijima S 1999 *Nature* **354** 56
[2] Satio R, Dresselhaus G D and Dresslhaus M S 1998 *Physical Properties of Carbon Nanotubes* (London: Imperial College Press)
[3] Wildoer J W G, Venema L C, Rinzler A G, Smalley R E and Dekker C 1998 *Nature* **391** 59
[4] Odom T W, Huang J L, Kim P and Lieber C M 1998 *Nature* **391** 62
[5] Mintmire J W, Dunlap B I and White C T 1992 *Phys. Rev. Lett.* **68** 631
Hamada N, Sawada S I and Oshiyama A 1992 *Phys. Rev. Lett.* **68** 1579
Satio R, Fujita M, Dresselhaus G and Dresselhaus M S 1992 *Appl. Phys. Lett.* **60** 2204
[6] Venema L C *et al* 1999 *Science* **283** 52
[7] Kim P, Odom T W, Huang J L and Lieber C M 1999 *Phys. Rev. Lett.* **82** 1225
[8] Carrol D L *et al* 1998 *Phys. Rev. Lett.* **81** 2332
[9] Meunier V, Senet P and Lambin Ph 1999 *Phys. Rev.* B **60** 7792
[10] Orlikowski D, Nardelli M B, Bernholc J and Roland C 2000 *Phys. Rev.* B **61** 14 194
[11] Chico L, Crespi V H, Benedict L X, Louie S G and Cohen M L 1996 *Phys. Rev. Lett.* **76** 971
[12] Kostyrko T, Bartkowiak M and Mahan G D 1999 *Phys. Rev.* B **59** 3214
[13] Igami M, Nakanishi T and Ando T 1999 *J. Phys. Soc. Japan* **68** 716
[14] Tersoff J and Hamann D 1983 *Phys. Rev. Lett.* **50** 1998
[15] Rubio A 1999 *Appl. Phys.* A **68** 275
[16] Xue Y Q and Datta S 1999 *Phys. Rev. Lett.* **83** 4844
[17] Meunier V and Lambin Ph 1998 *Phys. Rev. Lett.* **81** 5588
[18] Mintmire J W, Dunlap B I and White C T 1992 *Phys. Rev. Lett.* **68** 631
[19] Mahan G D 1990 *Many-Particle Physics* (New York: Plenum) ch 3
[20] Mintmire J W and White C T 1998 *Phys. Rev. Lett.* **81** 2506
[21] Choi H J, Ihm J, Louie S G and Cohen M L 2000 *Phys. Rev. Lett.* **84** 2917
[22] Satio R, Dresselhaus G D and Dresslhaus M S 1998 *Physical Properties of Carbon Nanotubes* (London: Imperial College Press) ch 4
[23] Yu M F, Lourie O, Dyer M J, Moloni K, Kelly T F and Ruoff R S 2000 *Science* **287** 637
[24] Walters D A *et al* 1999 *Appl. Phys. Lett.* **74** 3803